Early Ordovician Aguada de la Perdiz Formation, northern Chile – Stratigraphy, provenance and regional tectonic setting

Heinrich Bahlburg[1*], Christoph Breitkreuz[2]

[1]Institut für Geologie und Paläontologie, Universität Münster, Germany

[2]Institut für Geologie, Bergakademie Freiberg, Germany

*corresponding author, hbahlburg@uni-muenster.de;

Christoph.Breitkreuz@extern.tu-freiberg.de

Abstract

The Early Ordovician Aguada de la Perdiz Formation of northern Chile is one of the oldest unmetamorphosed sedimentary units in Chile. Graptolites indicate a late Floian to early Dapingian age of the formation at the Aguada de la Perdiz type locality and small nearby outcrops in Chile. Correlative outcrops on the Argentinian side occur at Huaitiquina, Filo Pircas, Sierra de Guayaos and Lever Mucar. Graptolites are associated with scarce occurrences of brachiopods and conodonts in some outcrops. In the Argentinian Puna the correlative units were assigned to the Coquena Formation. All outcrops consist mainly of volcaniclastic turbidite and ash-rich flow deposits with intercalations of bimodal lavas, volcanic breccias and reworked felsic tuffs. The lithological assemblage reflects deposition in a marine volcaniclastic apron located on the eastern flank of the Famatinian magmatic arc. We propose to collectively group all respective outcrops in the Aguada de la Perdiz Formation thus respecting precedence of its first definition by García et al. (1962) because of the common characteristics of the formation on both sides of the international border. New U–Pb detrital zircon ages of a sample (n=124) from the Huaitiquina locality range between 3530 and 550 Ma and reflect a common polycyclic provenance from older Amazonian sources. The youngest

IN PRESS

U–Pb zircon age corresponds to the Ediacaran and predates the biostratigraphically defined depositional age by ca. 80 Myr. Thus, the synsedimentary Famatinian felsic volcanism, otherwise common in coeval units, is not reflected in the detrital zircon age record at Huaitiquina. The absence of Famatinian ages may indicate that sediment delivery from the Famatinian arc line source bypassed this site and that erosion of the arc had locally dissected the volcanic edifices and had progressed to access the pre-Pampean Neoproterozoic arc basement.

Resumen

La Formación Aguada de la Perdiz (Ordovícico Temprano), norte de Chile – Estratigrafía, proveniencia y marco tectónico regional. La Formación Aguada de la Perdiz, del Ordovícico Temprano en el norte de Chile, constituye una de las unidades sedimentarias no metamorficas más antiguas del país. La presencia de graptolitos indica una edad comprendida entre el Floiano tardío y el Dapingiano temprano en la localidad tipo de Aguada de la Perdiz y en pequeños afloramientos próximos en territorio chileno. Afloramientos correlativos en el sector argentino se encuentran en Huaitiquina, Filo Pircas, Sierra de Guayaos y Lever Mucar. En algunos de estos afloramientos, los graptolitos se asocian a registros escasos de braquiópodos y conodontos. En la Puna argentina, las unidades correlativas han sido asignadas a la Formación Coquena. Todos los afloramientos están constituidos principalmente por turbiditas volcanoclásticas y depósitos de flujo ricos en ceniza, intercalados con lavas bimodales, brechas volcánicas y tobas félsicas retrabajadas. Este conjunto litológico refleja la depositación en un abanico submarino volcanoclástico emplazado en el flanco oriental del arco magmático famatiniano. Se propone agrupar colectivamente todos los afloramientos correspondientes bajo la denominación de Formación Aguada de la Perdiz, respetando la precedencia de su definición original por García et al.

IN PRESS

(1962), en virtud de las características comunes que la unidad presenta a ambos lados de la frontera internacional. Nuevas dataciones U–Pb en circones detríticos de una muestra (n=124) proveniente de la localidad de Huaitiquina registran edades comprendidas entre 3530 y 550 Ma, lo que refleja una procedencia policíclica común a partir de fuentes amazónicas más antiguas. La edad U–Pb más joven corresponde al Ediacárico y antecede en aproximadamente 80 millones de años a la edad de depositación definida mediante bioestratigrafía. De este modo, el vulcanismo félsico famatiniano sinsedimentario, común en unidades coetáneas, no se encuentra representado en el registro de circones detríticos de Huaitiquina. La ausencia de edades famatinianas podría indicar que el aporte sedimentario procedente del arco famatiniano no alcanzó este sector, y que la erosión del arco había disectado localmente los edificios volcánicos, permitiendo el acceso al basamento neoproterozoico pre-pampeano.

1. Introduction

The Late Cambrian to Silurian/Early Devonian accretionary Famatinian orogenic cycle (520-410 Ma) is the second cycle of the Terra Australis Orogen, the evolution of which started at ca. 650 Ma (Cawood, 2005). The Famatinian orogenic cycle is recorded along the present western margin of South America from ~36°S to the Mérida Andes of northern Venezuela at ~10°N. It is characterized along its entire length by major intrusive bodies formed in calc-alkaline magmatic arcs between 490 and 460 Ma (Rapela et al., 1990, 1998a, 2018; Pankhurst et al., 1998; Weinberg et al., 2018; see review in Ramos, 2018) (Fig. 1). Rocks metamorphosed at variable depths are abundant and outline a strong tectonic segmentation into exposures of different crustal levels (e.g., Willner et al., 1987; Otamendi et al., 2008; Ramos, 2018; Alasino et al., 2024). Unmetamorphosed or only slightly metamorphosed volcanic rocks are relatively

IN PRESS

scarce and occur only in those segments where upper crustal levels are exposed. These include relatively widespread occurrences in the Sierra de Famatina (e.g., Armas et al., 2018, 2021; Cisterna and Coira, 2022) and in the Puna of northern Chile and northwestern Argentina (e.g., Schwab, 1973; Breitkreuz, 1986; Coira and Barber, 1989; Coira and Nullo, 1989; Bahlburg, 1990, 1998; Coira et al., 2009a,b) (Fig. 1). Isolated occurrences are in the Cordillera Oriental of southern and central Peru (Haeberlin and Fontbotè, 2002; Bahlburg et al., 2006, 2011) and in the northern Venezuelan Andes (Ramos, 2018).

In this contribution we discuss the main upper crustal non-metamorphic occurrences of volcaniclastic successions in the Puna de Antofagasta of northern Chile and the northern Puna of northwestern Argentina (Figs. 1 and 2). They straddle the international border which impeded cross-border considerations and correlations. We present new detrital zircon U–Pb age data on a sample from the Huaitiquina outcrop on the Argentinian side. We consider the new detrital zircon age data jointly with similar data from the broadly coeval Complejo Ígneo-Sedimentario del Cordón de Lila (CISL; Niemeyer, 1989) (Fig. 1) in the Salar de Atacama basin to the west in order to clarify the regional implications of the new data for their host formations.

2. Stratigraphic framework of Ordovician units in the Puna of northern Chile and northwestern Argentina.

The Aguada de la Perdiz Formation was the first recognized stratigraphic unit of Ordovician age in Chile and is located in the Puna de Antofagasta of northern Chile. Together with the Early Ordovician sedimentary rocks of the CISL (Figs. 1 and 3) it is the oldest unmetamorphosed sedimentary unit on continental Chilean territory. Its base and top are unseen. The formation was first described and named by García et al.

IN PRESS

(1962) and was assigned to the Lower Ordovician Arenig Series (now Floian-Dapingian; Fig. 3) on the basis of graptolite finds. Additional graptolite fauna found at related outcrops in the vicinity (Poquis, Lever Mucar; Figs. 1 and 2a) led Pérez (1983) to group all these occurrences in the Aguada de la Perdiz Formation with a corresponding age range encompassing the Arenig and Llanvirn (now Floian to Darriwilian; Fig. 3; Table 1).

On the Argentinian side it was Schwab (1973) who first found upper Arenig (now Dapingian; Fig. 3; Table 1) graptolites at Filo Pircas in a succession of greywackes and shales with diabase intercalations (Figs. 1 and 2). He was the first who in this context suspected a volcanic origin also for the cherts ('pedernal'; García et al., 1962) of the upper Aguada de la Perdiz Formation and correlated his graptolite finds with those on the Chilean side. This was later substantiated with correlative finds in volcaniclastic strata in the Sierra de Guayaos near Catua (Aceñolaza and Durand, 1974; Coira et al., 1987) (Figs. 1 and 2A; Table 1) and, together with conodonts of the same age, at Huaitiquina (Monteros et al., 1996; Toro et al., 2019, 2020) (Table 1). Following Schwab (1973), the respective rocks on the Argentinian side were assigned to the Coquena Formation of Dapingian to Darriwilian age (e.g., Monteros et al., 1996; Toro et al., 2019, 2020) (Fig. 3; Table 1). Ordovician brachiopods confirming the age assignments indicated by the graptolites were found in similar rocks at several localities south of the study area (e.g., Benedetto, 2001, 2003). Bahlburg et al. (1990) presented additional graptolite data, further constraining the stratigraphic relationships between the Aguada de la Perdiz Formation and equivalents and the partly coeval and younger Ordovician turbidite units farther east in the Argentinian Puna (Figs. 1 and 3).

IN PRESS

Until recently, the Ordovician stratigraphic schemes of the Chilean and Argentinian Puna were kept almost completely separate. It was noted that the lower Coquena Formation (Fig. 3) contained volcanic and volcaniclastic rocks which were broadly coeval with the Aguada de la Perdiz Formation directly on the other side of the border in Chile (Schwab, 1973) but the schemes were not unified. To simplify matters, Bahlburg et al. (1990) combined all of the volcanic and volcaniclastic units of Floian to Darriwilian age of the Chilean and Argentinian Puna under the informal name Volcanosedimentary Successions of the Puna, for which we now suggest the name Aguada de la Perdiz Formation because it has precedence. As the respective volcanic record had, however, started already in the Tremadocian Las Vicuñas Formation (Moya et al., 1993), we combine here all Lower and Middle Ordovician volcanic and volcaniclastic units in the Puna Volcanic Complex, including the redefined Aguada de la Perdiz Formation (Fig. 3).

3. The original Aguada de la Perdiz Formation

Fuenzalida (1957) was the first to report the presence of Ordovician sedimentary rocks in the Puna of Antofagasta of northern Chile bearing the graptolite *Didymograptus sagitticaulis* at the Lever Mucar locality (Fig. 1; Table 1). The Aguada de la Perdiz Formation (Figs. 1-3) was established by García et al. (1962) who described a ~2000 m thick siliciclastic succession divided into two parts, a lower member of quartz-rich sandstones yielding the graptolites *Didymograptus* sp., *Tetragraptus quadribrachiatus* and *Tetragraptus approximatus*, and an upper member consisting mainly of cherts ('pedernal'; Fig. 3; Table 1). The formation is exposed at altitudes of 4400–4600 m a.s.l. at the eastern margin of the volcanoes of the Cordillera Occidental (Figs. 1 and 2). Marinovic (1979) and Pérez and Davidson (1982) added finds of *Glossograptus* sp. and *Isograptus* sp., among others (Table 1), at the isolated Poquis locality north of

IN PRESS

Aguada de la Perdiz (Fig. 1) and recognized the sedimentary rocks as a succession of turbidites. The summary of available graptolite data by Pérez (1983) was extended by Breitkreuz (1986) who reported a rather diverse graptolite fauna including *Didymograptus bifidus* (Table 1) which helped to place the Aguada de la Perdiz outcrop in the mid-Floian *bifidus* zone of the Lower Ordovician (Table 1). The combination of biostratigraphic data from the Chilean Aguada de la Perdiz, Poquis and Lever Mucar localities indicates a stratigraphic range of the Early and Middle Ordovician units from the mid-Floian into the Darriwilian (Arenig-Llanvirn of the British Series; Fig. 3, Table 1).

3.1 Depositional facies

Breitkreuz (1986) was the first to observe the volcanic nature of the Aguada de la Perdiz Formation at its type locality (Figs. 1, 2, 4, and 5A). He upheld the original division of the formation by García et al. (1962) into two members (Fig. 4). The lower coarse-grained member consists of a ~1500 m thick succession of red to multi-colored (Figs. 4 and 5B) volcaniclastic strata including felsic volcaniclastic debris flow deposits (Fig. 5B-D). It is overlain by the ~1200 m thick upper member of silicified, fine-grained and thin-bedded tuffs, reworked tuffs and mass flow deposits with colors ranging from greyish-black to brownish-yellow (Figs. 4, 5A, and 5E).

As summarized from Breitkreuz (1986) and Breitkreuz et al. (1989), the coarse-grained volcaniclastic rocks of the lower member consist of sandy-conglomeratic beds up to one meter thick, interspersed with thin, fine-sandy to pelitic, locally fossiliferous layers (Fig. 2B). Thick monomict and polymict breccia tuffs, reaching up to 15 m, are occasionally intercalated (Fig. 5B, C). The sandy-conglomeratic beds maintain a consistent lateral thickness and exhibit normal and coarse-tail grading (Fig. 5B).

IN PRESS

According to Breitkeuz (1986) and Breitkreuz et al. (1989) volcaniclastic sandstones display compaction structures including pressure solution and crystal deformation parallel to bedding planes alongside partial carbonate replacement. The matrix consists of fine-grained chert, with former glass shard outlines visible under the microscope in unpolarized light. The framework components, in decreasing abundance, include resorption-embayed quartz, sanidine, variably sericitized andesine/labradorite, devitrified pumice fragments. Fibrous cherts, and accessory minerals such as biotite (partly chloritized), opaques, and zircon complete the picture. Non-volcanic quartzite rock fragments occur in the conglomerates.

Breccia tuffs are intercalated in the lower member. They either consist of rhyolitic components including non-graded ash layers, or siliceous tuff clasts, reaching up to one meter in size, along with plastically deformed, laminated tuff rafts suspended in a trachytic tuff groundmass (Fig. 5C). Component size decreases rapidly toward the top of the breccia tuffs.

The composition of the breccia matrix includes basaltic hydroclastic fragments with vesicles and perlitic cracks suggesting proximal subaquatic magmatic activity. They occur jointly with aphanitic to intersertal volcanic fragments and siliceous tuff clasts compositionally similar to the larger breccia components. Similar sedimentary bodies have been described by White and Busby-Spera (1987) as deposits of 'short-distance, weakly turbulent, high-concentration sediment flows.'

The coarse-grained volcaniclastic deposits of the lower section of the formation lack evidence of a hot regime of transport and sedimentation including the absence of any

IN PRESS

208 indication of welding and fusion of particles. The succession is best characterized as
209 a thick stack of volcaniclastic turbidity current and debris flow deposits (Cas and
210 Wright, 1987).
211
212 The transition from the lower coarse-grained to the upper fine-grained member is
213 marked by a ~10 m thick fining- and thinning-upward sequence. The upper member
214 consists of 20–50 cm thick tuffs and reworked tuffs, the latter characterized by fine
215 cross beds, parallel and convolute lamination, and cut-and-fill structures deposited
216 from ash-bearing flows (White and Busby-Spera, 1987) (Figs. 4 and 5E). Less silicified,
217 thinly bedded siltstone and claystone intercalations locally contain graptolites and
218 phyllocarids (Breitkreuz, 1986).
219
220 Thin-section analysis of the tuffs reveals a fine-grained, devitrified groundmass with
221 remnants of former glass shards. Small amounts of quartz, feldspar, biotite, and chert
222 fragments are arranged in layers within this matrix. Patchy carbonatization is also
223 observed in some areas.
224
225 A few meter-thick mafic lavas occur in the formation. In the lower member they consist
226 of aphanitic to intersertal-textured rocks, primarily composed of variably altered
227 plagioclase and augite. The mafic lava in the upper part of the fine-grained section is
228 an altered basalt containing chalcedony- and carbonate-filled amygdales, along with
229 some feldspar phenocrysts.
230
231 3.2 Depositional environment
232 The depositional environment is interpreted as marine because of the presence of
233 graptolite-bearing strata (Pérez, 1983; Breitkreuz, 1986; Monteros et al., 1996). The

IN PRESS

234 preservation and abundance of turbidites indicates that the depositional site was below
235 storm wave base and at the base of some considerable relief conducive to the
236 formation of turbidity currents and debris flows.
237
238 The characteristics of lithology and facies suggest that the Aguada de la Perdiz
239 Formation represents a submarine volcaniclastic apron (White and Busby-Spera,
240 1987) of a mid-Floian (Fl3; Table 1) possibly subaerial chain of bimodal but
241 predominantly felsic volcanoes (Breitkreuz, 1986; Bahlburg, 1990). Periodically, this
242 apron experienced subaqueous lava extrusions indicating activity of nearby mafic
243 vents. While sporadic proximal felsic volcanic activity is indicated by a few massive
244 rhyolitic breccia tuffs, the dominance of turbidity current over debris flow deposits
245 suggests that the formation developed distally from the primary source of volcanic
246 debris. The extent to which air fall contributed to the deposition of the volcaniclastic
247 strata is unknown. Low-density turbidity currents and/or dilute, slow-moving ash-
248 bearing flows were responsible for forming submarine, rhythmic, fine-grained tuff
249 successions typical of the upper member of the Aguada de la Perdiz Formation (Figs.
250 4, 5A, and 5E).
251
252 **4. Correlative units in the neighbouring Puna of northwestern Argentina**
253 4.1 Huaitiquina
254 The Aguada de la Perdiz Formation at the Huaitiquina locality (Figs. 1 and 2) is
255 exposed at altitudes of 4200–4400 m a.s.l. The base of the section is formed by the
256 westernmost NNW-SSE striking anticline in the eastern part of the outcrop area. Along
257 a fault in the Río Huaitiquina valley there is a repetition of strata, which is accounted
258 for in figure 4. The top of the section is covered by Cenozoic rocks.
259

IN PRESS

Schwab (1973) characterized the strata of the Río Huaitiquina area as conglomeratic greywackes with intercalations of diabasic lavas and tuffs. Méndez et al. (1979) documented a 920 m thick section of intercalated clastic rocks and andesites which presumably represent the lower part of the exposed section (Figs. 4 and 6A). Coira and Barber (1987) divided the succession into five parts which, in their interpretation, mirror the evolution from andesitic to explosive siliceous and submarine arc volcanism, the latter of which is succeeded by epiclastic sedimentary rocks (Fig. 6B). The described section is 1100 m thick.

In detail the complete section begins with a ~500 m thick sequence of strongly jointed subaqueous vesicular basalt, basaltic andesite and andesite lavas and associated hydroclastic breccias (Fig. 6C, D). They are intercalated with mostly coarse-grained monomict mafic debris flow deposits with minor grading at the top and are overlain by polymict and felsic partly brecciated debris flow deposits (Fig. 6E) some of which contain rafts of deformed laminated siliceous tuffs up to one meter in diameter similar to the ones found at the Aguada de la Perdiz locality (cf. Fig. 5D). These give way to coarse and fine-grained volcaniclastic turbidites (Fig. 6F). Well sorted sandstones with 2-3 cm high symmetric wave ripples are intercalated at the top of this lower volcanic section (Figs. 4 and 6G).

The middle and upper part of the ~3300 m thick succession consists of volcaniclastic fine- to coarse-grained and partly graded sandy turbidites. Further basalt lavas are intercalated occasionally in the upper section and up to 40 m thick packages of 20–50 cm thick siliceous, laminated tuffs are common (cf. Fig. 5E). Some of the tuffs have a weakly erosive base. Massive and graded sandstones and pebbly sandstones are deposits from turbidity currents.

IN PRESS

286

287 4.2 Filo Pircas

288 The 660 m thick Filo Pircas section (FP; Figs. 1, 2, and 4) is exposed at an altitude of
289 4200–4400 m a.s.l., between a syncline in the west and an anticline in the east
290 (Bahlburg, 1990). 3–20 m thick successions of fine-grained and thin-bedded (10–50
291 cm) volcaniclastic turbidites (Fig. 5F, H) alternate with 5–20 m thick successions of thin
292 (5–15 cm) laminated tuffs which frequently have an erosional base (Fig. 5G, H).
293 Thickness and abundance of the tuffs decrease up section.

294

295 The outcrop at Lever Mucar (Fig. 1) represents an along-strike continuation of the Filo
296 Pircas section and appears to contain more epiclastic sandstones and shales in the
297 northern reaches of the outcrop (Coira and Nullo, 1989).

298

299 4.3 Nature of magmatism in the Aguada de la Perdiz Formation

300 Mafic volcanic arc lavas are most abundant in the lower member of the Aguada de la
301 Perdiz Formation and give way to more felsic volcanism up-section (Schwab, 1973;
302 Breitkreuz et al., 1989; Coira and Barber, 1989; Bahlburg, 1990) (Fig. 4). The
303 geochemical characteristics identify both mafic and felsic volcanic rocks as calc-
304 alkaline and related to the activity of the Ordovician Famatinian volcanic arc (Faja
305 Eruptiva de la Puna Occidental; Palma et al. 1986) above an east-dipping subduction
306 zone (present coordinates) along the evolving Famatinian accretionary orogen (Coira
307 et al., 1982, 1999, 2009b; Coira and Barber, 1987, 1989; Breitkreuz et al., 1989;
308 Bahlburg, 1990, 1998; Niemeyer et al., 2018; Ramos, 2018).

309

310 4.4 Depositional facies of the Huaitiquina and Filo Pircas localities and biostratigraphic
311 correlation to the Aguada de la Perdiz locality

IN PRESS

Submarine basalts and andesites and associated debris flow deposits characterize the lower 500 m of the Huaitiquina section. This mafic magmatism is associated with felsic tuffs which occur as extensive layers or reworked as rafts in the debris flow deposits. Lithologically related tuffs which lack the erosive base may have been connected to submarine effusions and may have been deposited from suspension (White and Busby-Spera, 1987). Similar to the Aguada de la Perdiz Formation at the type locality, the partly cross-bedded tuffs are interpreted to have a subaerial origin and were subsequently deposited in a marine environment by dilute slow-moving ash-rich flows.

Coira and Barber (1987) found thin stromatolites in the lower part of their section in the Huaitiquina area. The combination of (i) the stromatolites, (ii) wave rippled sandstones, and (iii) the sparse graptolite and conodont fauna (Monteros et al., 1996; Toro et al., 2020) (Table 1) indicates shallow marine conditions during deposition of the lower part of the Huaitiquina section. Volcaniclastic turbidites dominate up-section and point to an increase in water depth and subsidence of the marine depositional site through time.

The deposits of the Filo Pircas section document the increasing abundance up-section of volcaniclastic, predominantly fine sand turbidites and ash-rich flow deposits commonly with an erosional base (Fig. 4; Table 1). The Filo Pircas section is rather similar to the upper member of the Aguada de la Perdiz Formation at the type locality and may be a biostratigraphic equivalent to this member in the late Floian and lower Dapingian (Fig. 4; Table 1). It may also represent an equivalent of the finer grained upper part of the Huaitiquina section (Fig. 4; Table 1).

IN PRESS

Overall, the depositional environment of the Aguada de la Perdiz Formation is that of a volcaniclastic apron connected to the bi-modal Famatinian volcanic arc source. The arc was located to the west between the discussed outcrops and the CISL in the Salar de Atacama basin. The volcaniclastic Aguada de la Perdiz Formation formed on the back-arc flank (Breitkreuz, 1986; Palma et al., 1986; Bahlburg, 1990; Niemeyer et al., 2018) (Fig. 1). The facies differences between the Aguada de la Perdiz and Huaitiquina localities are likely due to a variable local input along the Famatinian magmatic arc source.

East of the discussed outcrops, at Filo Tropapete (Schwab, 1973) (Fig. 1), the strata of the Aguada de la Perdiz Formation pass gradually into the turbidite successions of the Lower Turbidite System (Coquena Formation; Schwab, 1973; Bahlburg, 1990) (Fig. 3). The Huaitiquina site records a marked deepening from shallow water depth with stromatolites to deeper subtidal depths at rates of up to 1100 m/Myr (Bahlburg, 1990), allowing the deposition of thick successions of turbidites. In view also of the accumulation of the Puna Turbidite Complex (Fig. 3) east of the Aguada de la Perdiz Formation, a deepening of the basin in eastward direction is inferred (Bahlburg, 1990).

The lithological development of the Filo Pircas section and the Filo Tropapete, and by correlation also of the upper sections at Aguada de la Perdiz and Huaitiquina, is interpreted to be the result of the waning of volcanic activity and the erosion of the volcanic edifices farther west during the upper Dapingian and the lower Darriwilian (Bahlburg, 1990) (Fig. 3).

5. New detrital zircon U–Pb ages of the Aguada de la Perdiz Formation

IN PRESS

362 Einhorn et al. (2015) presented a few reliable detrital zircon ages (n=9) obtained from
363 a detrital sedimentary sample of the Aguada de la Perdiz Formation at its type locality.
364 These ages range from ca. 476 to 465 Ma and include a youngest population with a
365 weighted mean age of 465 ± 4 Ma (lower Darriwilian; n=5) and a youngest zircon age
366 of 453 ± 12 Ma. Both are commensurate with the lower Darriwilian biostratigraphic age
367 of the formation. In order to further constrain and broaden the age and provenance
368 information on the Aguada de la Perdiz Formation we dated detrital zircon in a single
369 sandstone sample (HY19) from the Huaitiquina locality.
370
371 5.1 Methods
372 Zircons were analysed for U–Pb geochronology by LA-ICP-MS at the Institute for
373 Mineralogy at the University of Münster using a ThermoFisher Element2 mass
374 spectrometer coupled to a Photon Machines Analyte G2 Excimer laser. The specific
375 procedural details are reported in a large number of studies including Kooijman et al.
376 (2012) and Bahlburg et al. (2016, 2020).
377
378 The zircons consist predominantly of euhedral, elongate or short prismatic as well as
379 subrounded to rounded grains usually less than 150 µm in length. The
380 cathodoluminescence images show oscillatory or sector zoning interpreted as of
381 magmatic origin; unzoned grains or those with irregular and round zoning are
382 considered to be of metamorphic origin (Vavra et al., 1999). Zircon rims were
383 preferentially analyzed to date the last growth stage of each zircon.
384
385 We uniformly apply a concordance filter of 90 and 101% to all our data (see
386 Supplementary Table 1) with 124 U–Pb ages fulfilling this criterion. 120 age dates have
387 errors between 1 and 5 %, averaging 2.3 %. For zircons older than 1.5 Ga the

IN PRESS

388 $^{207}Pb/^{206}Pb$ ages are used and for those younger the $^{206}Pb/^{238}U$ ages are preferred.
389 We follow Spencer et al. (2016) who evaluated the error dimensions of 38,000
390 published zircon ages and recommended the crossover point from $^{207}Pb/^{206}Pb$ ages to
391 $^{206}Pb/^{238}U$ ages be placed at 1.5 Ga. Kernel Density Estimates (KDE) were calculated
392 with the *provenance* software package (Vermeesch et al., 2016).
393
394 5.2 Results
395 The detrital zircon U–Pb ages of sample HY19 from the middle part of the Huaitiquina
396 section (Fig. 4) range between 3529±31 Ma and 552±9 Ma (Supplementary Table 1).
397 Major abundance maxima are at ca. 1550, 1480, and 1060 Ma, with minor ones at ca.
398 1760 and 650 Ma (Fig. 7). Multiple studies have demonstrated an Amazonian and
399 proto-Andean origin of the detritus constituting the (Early) Paleozoic sedimentary rocks
400 of the Andean region (e.g., Willner et al., 2008; Bahlburg et al., 2009, 2011, 2025;
401 Augustsson et al., 2015; Einhorn et al., 2015; Pankhurst et al., 2016). The listed
402 maxima can be apportioned to the major orogenic and tectonic cycles reflecting the
403 crustal evolution of Amazonia since the beginning of the Paleoproterozoic with
404 individual zircon ages extending back to the Paleoarchean (e.g., Cawood, 2005;
405 Cordani and Teixeira, 2007; Pepper et al., 2016; Bahlburg et al., 2025) (Fig. 7).
406
407 In decreasing order of abundance, the Huaitiquina sample (Fig. 7) includes 27 % of
408 grains linking back to the Rondonia-San Ignacio orogenic cycle (1550–1200 Ma), 26
409 % to the Sunsás cycle (1200–1000 Ma), 21 % to the Río Negro-Juruena cycle (1800–
410 1550 Ma), 9 % to the phase of Neoproterozoic rifting connected to the breakup of
411 Rodinia (1000–650 Ma; Cawood et al., 2016; Bahlburg et al., 2020), 6 % to the Central
412 Amazonian Province (>2300 Ma), 5 % to the Ventuari-Tapajos cycle (2000–1800 Ma),
413 and 3 % each to the Maroni-Itacaiunas (2300–2000 Ma) and the Olmos-Pampean

IN PRESS

cycles (650–520 Ma; Cordani and Teixeira, 2007; Bahlburg et al., 2025) (Fig. 7). There are no syndepositional Ordovician detrital zircon ages. The age spectrum is thus dominated by Paleo- and Mesoproterozoic ages recording the evolution of the Terra Amazonica Orogen (Bahlburg et al., 2025) (Fig. 7).

The youngest age peak is represented by two grains giving an average mean age of 652 Ma (Fig. 7). The three youngest ages between 629 and 552 Ma are from weakly rounded subidiomorphic zircon grains (see Supplementary Figure 1). The maximum likelihood age of deposition calculated from the entire sample according to Vermeesch (2021) is 565±18 Ma.

Surprisingly, at Huaitiquina there are no detrital zircon ages reflecting the synsedimentary volcanic activity recorded by the mafic and felsic volcanic rocks intercalated in the Aguada de la Perdiz Formation (see above; Coira and Barber, 1987, 1989; Breitkreuz et al., 1989; Bahlburg, 1990, 1998; Coira et al., 1999, 2009b). The Cryogenian–Ediacaran (Neoproterozoic) maximum likelihood age of deposition (Vermeesch, 2021) of 565±18 Ma derived from the detrital zircon age spectrum is older by ca. 100 Myr than the actual Early Ordovician biostratigraphic age of deposition (Fig. 3; Table 1).

The detrital zircon U–Pb age spectrum of the Aguada de la Perdiz Formation at the Huaitiquina location reflects the expected Precambrian Amazonian provenance found in many studies throughout the Andes. In contrast, the absence of synmagmatic Ordovician ages reflecting the syndepositional volcanic activity together with the presence of Cryogenian–Ediacaran youngest ages is an unexpected result. The youngest magmatic event recorded by the data from Huaitiquina is the alleged Olmos

IN PRESS

magmatic arc in eastern Peru active between 650 and 550 Ma (Chew et al., 2008; Bahlburg et al., 2025) and before the onset of the Pampean orogenic cycle (540-520 Ma; Rapela et al., 1998a,b). However, the few detrital zircon U–Pb ages obtained from the formation at the Aguada de la Perdiz location constrain the age of the sampled layer at 465±4 Ma (lower Darriwilian; n=5; Einhorn et al., 2015). Similar ages are also abundant farther west in the CISL (Figs. 1 and 7). This indicates that sediment routing systems from the Famatinian magmatic arc in fact delivered Famatinian detritus to the considered formations. They appear, however, to have bypassed the Huaitquina locality.

Detrital zircon age spectra of the Ediacaran–Early Cambrian siliciclastic Puncoviscana Formation involved in the formation of the Pampean orogenic cycle in northwestern Argentina (Ramacciotti et al., 2025) show age distributions similar to the Huaitiquina sample. The detritus recorded in sample HY19 could therefore have been derived from reworking of the Puncoviscana rocks. However, both the position of the Aguada de la Perdiz Formation on the eastern flank of the Famatinian magmatic arc and the east-directed paleocurrent and eastward deepening facies trends of the Ordovician basin in the Puna of Argentina make a provenance from the Puncoviscana formation from eastern side of the basin unlikely.

The coeval magmatism of the Faja Eruptiva de la Puna Oriental in the eastern Puna and east of the Puna Volcanic Complex (Coira et al., 1999; Bahlburg et al., 2016; Pankhurst et al., 2016) (Fig. 1) is also not registered at the Huaitiquina locality. This is probably due to the deeper Early Ordovician basin between this magmatic zone and the Aguada de la Perdiz Formation which may have captured the syndepositional magmatic detritus derived from the east (Bahlburg, 1990).

IN PRESS

The data also indicate that the youngest detritus included in the Lower Ordovician siliciclastic deposits at Huaitiquina predominantly reflects a potentially polycyclic derivation from sources older by 100 to 200 Myr, having bypassed Pampean sources of 540–520 Ma (Rapela et al., 1998a,b).

6. Discussion and Conclusions

The Puna Volcanic Complex is separated into two parts by the diachronous angular Tumbaya unconformity (Moya, 2015) (Fig. 3). Units below this unconformity include the Las Vicuñas Formation north of the Salar del Rincón (Moya et al., 1993) and the CISL in northern Chile (Niemeyer, 1989) (Fig. 1), both belonging to the Tremadocian (Fig. 3). The Aguada de la Perdiz Formation was deposited above the unconformity, with an upper Floian to lower Darriwilian age. At the type locality this biostratigraphic age coincides with very scarce detrital zircon age data between 475 and 465 Ma.

The Quebrada Grande Formation in the Cordón de Lila in northern Chile overlies the CISL unconformity and has a Darriwilian biostratigraphic age based on brachiopods and graptolites (González et al., 2007) (Fig. 1; Table 1). However, the CISL and the Quebrada Grande and Aguada de la Perdiz formations have very similar depositional ages as defined by U-Pb zircon age data. The youngest age cluster obtained from the CISL turbidites yielded a weighted mean age of 477±5 Ma with a youngest zircon age of 475±11 Ma (Augustsson et al., 2015). Rhyolite and dacite lava intercalations gave ages between 480 and 470 Ma (Zimmermann et al., 2010; Pankhurst et al., 2016). Coeval intrusive activity is recorded in the Cordón de Lila between 485 and 471 Ma (Pankhurst et al., 2016) (Fig. 1). The Quebrada Grande Formation equally includes rhyolite and dacite lava flows dated at ca. 480, 477 and 470 Ma in its lower part

IN PRESS

(Zimmermann et al., 2010; Pankhurst et al., 2016) (Fig. 3). Pampean detrital zircon ages are scarce here as well but those reflecting the Olmos magmatic arc between 650 and 550 Ma are abundant with a peak age at ca. 640 Ma (Augustsson et al., 2015). Considering both the biostratigraphic and detrital zircon U–Pb ages of the Aguada de la Perdiz Formation, the CISL and the Quebrada Grande Formation, the differences between all three formations in physical stratigraphy and biostratigraphy can presently not be reproduced or resolved by the available geochronological data.

The depositional environment accommodating the variable lithologies of the Aguada de la Perdiz Formation can best be described as a volcaniclastic apron which formed on the eastern flank of the Famatinian magmatic arc which in this region is also named Faja Eruptiva de la Puna Occidental (Palma et al., 1986; Bahlburg, 1990; Coira et al., 2009b).

The sandstones and greywackes of all formations constituting the Puna Volcanic Complex are predominantly compositionally immature and uniformly rich in feldspar and rock fragments. They have a rhyodacitic to rhyolitic upper crustal geochemical composition similar to magmatic arcs (Bahlburg, 1998; Zimmermann and Bahlburg, 2003; Zimmermann et al., 2010; Zimmermann, unpublished data on the Las Vicuñas Formation).

There are notable differences between the detrital zircon U–Pb age spectra of the CISL and the Aguada de la Perdiz Formation at the Huaitiquina locality. The distribution of ages and their abundances in samples of both formations reflect an expected Precambrian Amazonian provenance previously also obtained in many sandstone studies throughout the Andes (e.g., Willner et al., 2008; Bahlburg et al., 2009, 2011,

IN PRESS

2025; Augustsson et al., 2015; Einhorn et al., 2015; Pankhurst et al., 2016). An unexpected result is the absence of synmagmatic Ordovician ages and the presence of Ediacaran youngest ages in the Huaitiquina sample (Figs. 3 and 7). The youngest magmatic event recorded by the Huaitiquina data is the inferred Olmos magmatic arc in eastern Peru active between 650 and 550 Ma (Chew et al., 2008; Bahlburg et al., 2025) and before the onset of the Pampean orogenic cycle (Rapela et al., 1998a,b). Famatinian zircons are present at the Aguada de la Perdiz type locality (Einhorn et al., 2015) but absent from the Huaitquina locality where Olmos-Pampean ages form the youngest age population (Fig. 7). The variable age distributions indicate that erosion in the region of the Famatinian arc source supplied detritus unevenly to the various depositional sites and that it had locally dissected the volcanic edifices to progressively access the arc basement.

Acknowledgements

We are indebted to Professor Francisco Hervé for his friendship and cooperation in many projects. Extended amicable discussions of the geology of the Andes over almost 40 years were spent sharing many a Pisco Sour and Chilean wine. We commend Jörg Maletz, Berlin, for his exhaustive reconsideration of pertinent graptolite data. The analysis of detrital zircon U–Pb ages was facilitated by J. Berndt and B. Schmitte at Institut für Mineralogie, Universität Münster, and was made possible by grant BA 1011/45-1 of the German Research Foundation (DFG) to HB. We appreciate the constructive reviews by Clara Cisterna, Luisa Pinto and Carlos Ramacciotti, and the editorial guidance by Robert Pankhurst and Daniel Bertin.

References

IN PRESS

Aceñolaza, F.G.; Baldis, B. 1987. The Ordovician system of South America. Correlation chart and explanatory notes. International Union of Geological Sciences Publication 22: 68 pp.

Aceñolaza, F.G.; Durand, F.R. 1975. Fauna graptolitica de Catua, provincias de Salta-Jujuy. I. Congreso Argentino de Paleontología y Bioestratigrafía Actas 1: 77-89.

Alasino, P.H.; Larrovere, M.A.; Ratschbacher, B.C.; Casquet, C.; Paterson, S.R. 2024. Famatinian magmatism in the SW Gondwana margin: A review focused on the Sierras Pampeanas (Argentina). Journal of South American Earth Sciences 145: 105035.

Armas, P.; Cristofolini, E.; Escribano, F.; Camilletti, G.; Barzola, M.; Otamendi, J.; Cisterna, C.; Leisen, M.; Romero, R.; Barra, F.; Tibaldi, A. 2021. Lower-middle Ordovician sedimentary environment and provenance of the Suri formation in the northern region of the Famatina belt, Catamarca, Argentina. Journal of South American Earth Sciences 105: 102948.

Armas, P.; Cristofolini, E.A.; Otamendi, J.E.; Tibaldi, A.M.; Barzola, M.G.; Camilletti, G.C. 2018. Geochronology and facies analysis of subaqueous volcanism of lower ordovician, Famatinian arc, Argentina. Journal of South American Earth Sciences 84: 255–265.

Augustsson, C.; Rüsing, T.; Niemeyer, H.; Kooijman, E.; Berndt, J.; Bahlburg, H.; Zimmermann, U. 2015. 0.3 b.y. of drainage stability along the Palaeozoic palaeo-Pacific Gondwana margin - a detrital zircon study. Journal of the Geological Society, London, 172: 186-200.

Bahlburg, H. 1990. The Ordovician basin in the Puna of NW Argentina and N Chile: geodynamic evolution from back-arc to foreland basin. Geotektonische Forschungen 75: 1-107.

Bahlburg, H. 1998. The geochemistry and provenance of Ordovician turbidites in the Argentinian Puna. *In* The Proto-Andean Margin of Gondwana (Pankhurst, R.J.; Rapela, C.W.; editors). Geological Society, London, Special Publication 142: 127-142.

IN PRESS

574 Bahlburg, H.; Berndt, J.; Gerdes, A. 2016. The ages and tectonic setting of the Faja Eruptiva de la Puna
575 Oriental, Ordovician, NW Argentina. Lithos 256-257: 41-54.
576
577 Bahlburg, H.; Breitkreuz, C.; Maletz, J.; Moya, M.C.; Salfity, J.A. 1990. The Ordovician sedimentary
578 rocks in the northern Puna of Argentina and Chile: New stratigraphical data based on graptolites.
579 Newsletters on Stratigraphy 23: 69-89.
580
581 Bahlburg, H.; Carlotto, V.; Cárdenas, J. 2006. Ollantaytambo Formation and Umachiri beds: evidence
582 of Late Cambrian to Ordovician arc volcanism in the Cordillera Oriental and Altiplano of southern Peru.
583 Journal of South American Earth Sciences 22: 52-65.
584
585 Bahlburg, H.; Kemp, A.I.S.; Fanning, C.M.; Martin, L. 2025. The Hf and O isotope record of long-lasting
586 accretionary orogens: The example of the Proterozoic and Paleozoic-Triassic central South America.
587 Earth-Science Reviews 262: 105068.
588
589 Bahlburg, H.; Vervoort, J.D.; Du Frane, S.A.; Bock, B.; Augustsson, C. 2009. Timing of accretion and
590 crustal recycling at accretionary orogens: Insights learned from the western margin of South America.
591 Earth-Science Reviews 97: 227-253.
592
593 Bahlburg, H.; Vervoort, J.D.; DuFrane, A.; Carlotto, V.; Reimann, C.; Cárdenas, J. 2011. The U–Pb and
594 Hf isotope evidence of detrital zircons of the Ordovician Ollantaytambo Formation, southern Peru, and
595 the Ordovician provenance and paleogeography of southern Peru and northern Bolivia. Journal of South
596 American Earth Sciences 32: 196-209.
597
598 Bahlburg, H.; Zimmermann, U.; Matos, R.; Berndt, J.; Jiménez, N.; Gerdes, A. 2020. The missing link of
599 Rodinia break up in western South America: A petrographical, geochemical, and zircon Pb-Hf isotope
600 study of the volcanosedimentary Chilla beds (Altiplano, Bolivia). Geosphere 16: 619-645.
601
602 Benedetto, J.L. 2001. Una fauna de braquiópodos arenigianos (Ordovfcico temprano) en rocas
603 volcanoclasticas de la Puna occidental de Argentina: implicaciones paleoclimáticas y paleogeográficas.
604 Ameghiniana 38, 131-146.

IN PRESS

Benedetto, J.L. 2003. The Ordovician brachiopod faunas of Argentina. *In* J.L. Benedetto, (Ed.): Ordovician fossils of Argentina. Secretaria de Ciencia y Tecnología, Universidad Nacional de Córdoba: 21 pp.

Benedetto, J.L.; Niemeyer, H.; González, J.; Brussa, E.D. 2008. Primer registro de braquiópodos y graptolitos ordovícicos en el Cordón de Lila (Puna de Atacama), norte de Chile. Ameghiniana 45: 3-12.

Breitkreuz, C. 1986. Das Paläozoikum in den Kordilleren Nordchiles (21°-25°S). Geotektonische Forschungen 70: 1-88.

Breitkreuz, C.; Bahlburg, H.; Delakowitz, B.; Pichowiak, S. 1989. Volcanic events in the Paleozoic central Andes. Journal of South American Earth Sciences 2: 171-189.

Brussa, E.D.; Toro, B.A.; Vaccari, N.E. 2008. Bioestratigrafía del Paleozoico Inferior en el ámbito de la Puna. *In* Geología y recursos naturales de la Província de Jujuy (Coira, B.; Zappettini, E.O.; editors). Relatorio del XVII Congreso Geológico Argentino: 93-97.

Cas, R.; Wright, J.V. 1987: Volcanic successions: modern and ancient. Allen & Unwin, London, 1-528.

Cawood, P.A. 2005. Terra Australis Orogen: Rodinia breakup and development of the Pacific and Iapetus margins of Gondwana during the Neoproterozoic and Paleozoic. Earth-Science Reviews 69: 249-279.

Cawood, P.A.; Strachan, R.A.; Pisarevsky, S.A.; Gladkochub, D.P.; Murphy, J.B. 2016. Linking collisional and accretionary orogens during Rodinia assembly and breakup: Implications for models of supercontinent cycles. Earth and Planettary Science Letters 449: 118-126.

Chew, D.M.; Magna, T.; Kirkland, C.L.; Mišković, A.; Cardona, A.; Spikings, R.A.; Schaltegger, U. 2008. Detrital zircon fingerprint of the Proto-Andes: Evidence for a Neoproterozoic active margin? Precambrian Research 167: 186–200.

IN PRESS

Cisterna, C.E.; Coira, B. 2022. Ordovician submarine to subaerial volcanism along the western Gondwana margin: records of the Famatinian belt evolution, north-western Sierras Pampeanas, Argentina. International Journal of Earth Sciences 111: 675–701.

Cohen, K.M.; Finney, S.C.; Gibbard, P.L. Fan, J.-X. 2013, updated. The ICS International Chronostratigraphic Chart. Episodes 36: 199-204.
http://www.stratigraphy.org/ICSchart/ChronostratChart2023-09.pdf

Coira, B.; Barber, E. 1987. Vulcanismo submarino Ordovícico (Arenigiano-Llanvirniano) del Rio Huaitiquina, Provincia de Salta, Argentina. X. Congreso Geológico Argentino Actas 4: 305-307.

Coira, B.; Barber, E. 1989. Vulcanismo submarino Ordovícico (Arenigiano-Llanvirniano) del Rio Huaitiquina, Provincia de Salta, Argentina. Revista de la Asociación Geologica Argentina 44: 68-77.

Coira, B.; Nullo, F. 1989. Facies piroclásticas del vulcanismo Ordovícico (Arenigiano-Llanvirniano), Salina de Jama, Jujuy. Revista de la Asociación Geologica Argentina 44: 89-95.

Coira, B.; Davidson, J.; Mpodozis, C.; and Ramos, V. 1982. Tectonic and magmatic evolution of the Andes of northern Argentina and Chile. Earth-Science Reviews 18: 303-332.

Coira, B.; Kay, S.M.; Peréz, B.; Woll, B.; Hanning, M.; Flores, P. 1999. Magmatic Sources and tectonic Setting of Gondwana Ordovician Magmas, Northern Puna of Argentina and Chile. *In* Laurentia-Gondwana connections before Pangaea. (Ramos, V.A.; Keppie, J.D.; editors). Geological Society of America Special Paper 336: 145-170.

Coira, B.; Kirschbaum, A.; Hongn, F.; Pérez, B.; Menegatti, N. 2009a. Basic magmatism in northeastern Puna, Argentina: Chemical composition and tectonic setting in the Ordovician back-arc. Journal of South American Earth Sciences 28: 374–382.

IN PRESS

Coira, B.; Koukharsky, M.; Perez, A. 1987. Rocas volcaniclásticas ordovícicas de la Sierra de Guayaos, Provincia de Salta, Argentina. X. Congreso Geológico Argentino Actas 4: 312-315.

Coira, B.; Koukharsky, M.; Ribeiro Guevara, S.; Cisterna, C.E. 2009b. Puna (Argentina) and northern Chile Ordovician basic magmatism - A contribution to the tectonic setting. Journal of South American Earth Sciences 27: 24–35.

Cordani, U.G.; Teixeira, W. 2007. Proterozoic accretionary belts in the Amazonian Craton. *In* Hatcher, R.D.; Jr.; Carlson, M.P.; McBride, J.H.; and Martínez Catalán, J.R.; eds.; 4-D Framework of Continental Crust. Geological Society of America Memoir 200: 297–320.

Einhorn, J.C.; Gehrels, G.E.; Vernon, A.; DeCelles, P.G. 2015. U–Pb zircon geochronology of Neoproterozoic–Paleozoic sandstones and Paleozoic plutonic rocks in the Central Andes (21°S–26°S). *In* Geodynamics of a Cordilleran Orogenic System: The Central Andes of Argentina and Northern Chile. (DeCelles, P.G.; Ducea, M.N.; Carrapa, B.; Kapp, P.A.; editors). Geological Society of America Memoir 212: 115–124.

Fuenzalida, H. 1957. Pizarras y cuarcitas de la localidad de Mucar. *In* Hoffstetter, R.; Fuenzalida, H, Cecioni, G.; 1957. Chile. Léxique Stratigraphique International, Vol. V, Amérique Latin, Fascule 7: 238.

García, A.F.; Perez D'Angelo, E.; Ceballos, S.E. 1962. El Ordovícico de Aguada de la Perdiz, Puna de Atacama, provincia de Antofagasta. Revista Mineralógica 77: 52-61.

Goldman, D.; Leslie, S.A.; Liang, Y.; Bergström, S.M. 2023. Ordovician biostratigraphy: index fossils, biozones and correlation. Geological Society, London, Special Publications 532: 31-62.

González, J.; Niemeyer, H.; Benedetto, J.L.; Brussa, E.D. 2007. The Ordovician Quebrada Grande Formation, Cordón de Lila (Antofagasta Region, northern Chile): stratigraphic and palaeogeographic significance. Revista Geológica de Chile 34: 277–290.

IN PRESS

Gutierrez-Marco, J.C.; Aceñolaza, G.F.; Esteban, S.B. 1996. Revision de algunas localidades con graptolitos ordovícicos en la Puna salto-jujeña (noroeste de Argentina). 12° Congreso Geológico de Bolivia (Tarija), Memorias 2: 725-731.

Haeberlin, Y.; Fontboté, L. 2002. The Eastern Cordillera of northern Peru, the remains of a lower Paleozoic collisional belt: new evidence from the Pataz region (7°40'-8°10'S). *In* Geological and structural setting, age, and geochemistry of the orogenic gold deposits at the Pataz Province, Eastern Andean Cordillera, Peru (Haeberlin, Y.; editor). Terre & Environnement 36: 21-48.

Kooijman, E.; Berndt, J.; Mezger, K. 2012. U–Pb dating of zircon by laser ablation ICP-MS: Recent improvements and new insights. European Journal of Mineralogy 24: 5-21.

Marinovic, N. 1979. Geología de los cuadrangulos Zapaleri y Nevados de Poquis, II. Región Chile. Memoria de Título (Unpublished), Universidad de Chile, Departamento de Geología: 75 p.

Méndez, V.; Turner, J.C.M.; Navarini, A.; Amengual, R.; Viera, V. 1979. Geología de la región noroeste, Provincias Salta y Jujuy, República Argentina. Dirección General de Fabricaciones Militares: 118 pp.

Monteros, J.A.; Moya, M.C.; Monaldi, C.R. 1996. Graptofaunas arenigianas en el borde occidental de Ja Puna argentina. Implicancias paleogeográficas. 12° Congreso Geológico de Bolivia (Tarija), Memorias 2: 733-746.

Moya, M.C. 2015. La "Fase Oclóyica" (Ordovícico Superior) en el noroeste argentino. Interpretación histórica y evidencias en contrario. Serie Correlación Geológica 31: 73-110.

Moya, M.C.; Malanca, S.; Hongn, F.D.; Bahlburg, H. 1993. El Tremadoc temprano en la Puna occidental argentina. XI. Congreso Geológico Argentino y II. Congreso de Exploración de Hidrocarburos Actas II, 20-30.

Niemeyer, H. 1989. El complejo igneo-sedimentario del Cordón de Lila, región de Antofagasta: Significado tectónico. Revista Geológica de Chile 16: 163-181.

IN PRESS

727

728 Niemeyer, H.; Götze, J.; Sanhueza, M.; Portilla, C. 2018. The Ordovician magmatic arc in the northern
729 Chile- Argentina Andes between 21° and 26° south latitude. Journal of South American Earth Sciences
730 81: 204-214.

731

732 Otamendi, J.E.; Tibaldi, A.M.; Vujovich, G.I.; Vinao, G. 2008. Metamorphic evolution of migmatites
733 from the deep Famatinian arc crust exposed in sierras Valle Fertil–La Huerta, San Juan, Argentina.
734 Journal of South American Earth Sciences 25: 313–335.

735

736 Palma, M.A.; Parica, P.D.; Ramos, V.A. 1986. El granito de Archibarca: Su edad y significado tectónico,
737 provincia de Catamarca. Revista de la Asociación Geológica Argentina 41: 414-419.

738

739 Pankhurst, R.J.; Hervé, F.; Fanning, M.C.; Calderón, M.; Niemeyer, H.; Griem-Klee, S.; Soto, F. 2016.
740 The pre-Mesozoic rocks of northern Chile: U–Pb ages, and Hf and O isotopes. Earth-Science Reviews
741 152: 88–105.

742

743 Pankhurst, R.J.; Rapela, C.W.; Saavedra, J.; Baldo, E, Dahlquist, J.; Pascua, I.; Fanning, C.M. 1998.
744 The Famatinian magmatic arc in the central Sierras Pampeanas: an Early to Mid-Ordovician continental
745 arc on the Gondwana margin. *In* The Proto-Andean Margin of Gondwana (Pankhurst, R. J.; Rapela, C.
746 W.; editors). Geological Society, London, Special Publication 142: 343-367.

747

748 Pepper, M.; Gehrels, G.; Pullen, A.; Ibanez-Mejia, M.; Ward, K.M.; Kapp, P. 2016. Magmatic history and
749 crustal genesis of western South America: Constraints from U-Pb ages and Hf isotopes of detrital zircons
750 in modern rivers. Geosphere 12: 1–24.

751

752 Pérez, E. 1983. Estado actual del conocimiento del Cambro-Ordovícico en Chile. *In* Desarrollo del
753 Cambrico y Ordovícico de Latino America. II. Reunión del Programa Internacional de Correlación
754 Geológica Projecto 192: 88-97.

755

756 Pérez, E.; Davidson, J. 1982. Turbiditas ordovícicas en la Puna de Antofagasta, Chile: consideraciones
757 paleogeográficas. Congreso Geológico Chileno 3, Resúmenes: 21-22.

IN PRESS

Ramacciotti, C.D.; Larrovere, M.A.; Casquet, C.; Lembo Wuest, C.I.; Morales Cámera, M.M.; Alasino, P.H.; Murra, J.A.; Riveros, A.; Basei, M.A.S.; Herazo, L.; Baldo, E.G. 2025. The Ediacaran margin of the Proterozoic MARA block and the sedimentary basins of the Clymene Ocean: Insights from U-Pb zircon geochronology in the Puna-Sierras Pampeanas transition, NW Argentina. Precambrian Research 422: 107792.

Ramos, V.A. 2018, The Famatinian Orogen along the protomargin of Western Gondwana: Evidence for a nearly continuous Ordovician magmatic arc between Venezuela and Argentina: *In* A. Folguera et al. (eds.), The Evolution of the Chilean-Argentinean Andes, Springer Earth System Sciences: 133-161.

Rapela, C.W.; Pankhurst, R.J.; Casquet, C.; Baldo, E.; Saavedra, J.; Galindo, C.; Fanning, C.M. 1998a. The Pampean Orogeny of the southern proto-Andes: Cambrian continental collision in the Sierras de Córdoba: *In* The Proto-Andean Margin of Gondwana (Pankhurst, R.J.; Rapela, C.W.; editors). Geological Society, London, Special Publication 142: 181-217.

Rapela, C.W.; Pankhurst, R.J.; Casquet, C.; Baldo, E.; Saavedra, J.; Galindo, C. 1998b. Early evolution of the Proto-Andean margin of South America. Geology 26: 707-710.

Rapela, C.W.; Pankhurst, RJ.; Casquet, C.; Dahlquist, J.A.; Fanning, C.M.; Baldo, E.G.; Galindo, C.; Alasino, P.H.; Ramacciotti, C.D.; Verdecchia, S.O.; Murra, J.A.; Basei, M.A.S. 2018. A review of the Famatinian Ordovician magmatism in southern South America: evidence of lithsophere reworking and continental subduction in the early proto-Andean margin of Gondwana. Earth-Science Reviews 187: 259-285.

Rapela, C.W.; Toselli, A.; Heaman, L.; Saavedra, J. 1990. Granite plutonism in the Sierras Pampeanas; an inner cordilleran Paleozoic arc in the southern Andes. *In* Plutonism from Antarctica to Alaska (Mahlburg Kay, S.; Rapela, C.W.; editors). Geological Society of America Special Paper 241: 77-90.

Schwab, K. 1973. Die Stratigraphie in der Umgebung des Salar de Cauchari (NW Argentinien). Ein Beitrag zur erdgeschichtlichen Entwicklung der Puna. Geotektonische Forschungen 43: 1-168.

IN PRESS

Spencer, C.J.; Kirkland, C.L.; Taylor, R.J.M. 2016. Strategies towards statistically robust interpretations of *in situ* U–Pb zircon geochronology. Geoscience Frontiers 7: 581-589.

Toro, B.A.; Herrera Sánchez, N.C. 2019. Stratigraphical distribution of the Ordovician graptolite *Azygograptus* Nicholson & Lapworth in the Central Andean Basin (northwestern Argentina and southern Bolivia). Comptes Rendus Palevol 18: 493-507.

Toro, B.A.; Heredia, S.; Herrera Sánchez, N.C.; Moreno, F.; Lo Valvo, G. 2019. First conodonts record in the Argentine Puna related to Middle Ordovician graptolites. Publicación Electrónica de la Asociación Paleontológica Argentina 19: R82-R83.

Toro, B.A.; Heredia, S.; Herrera Sánchez, N.C.; Moreno, F. 2020. First Middle Ordovician conodont record related to key graptolites from the western Puna, Argentina: Perspectives for an integrated biostratigraphy and correlation of the Central Andean Basin. Andean Geology 47: 144-161.

Vavra, G.; Schmid, R.; and Gebauer, D. 1999. Internal morphology, habit and U-Th-Pb microanalysis of amphibolite-to-granulite facies zircons: geochronology of the Ivrea Zone (Southern Alps). Contributions to Mineralogy and Petrology 134, 380–404.

Vermeesch, P. 2021. Maximum depositional age estimation revisited. Geoscience Frontiers 12: 843-850.

Vermeesch, P.; Resentini, A.; Garzanti, E. 2016. An R package for statistical provenance analysis. Sedimentary Geology 336: 14-25.

Weinberg, R.F.; Becchio, R.; Farias, P.; Suzaño, N.; Sola, A. 2018. Early Paleozoic accretionary orogenies in NW Argentina: Growth of West Gondwana. Earth-Science Reviews 187: 219–247.

White, J.D.L.; Busby-Spera, C. 1987. Deep marine arc apron deposits and syndepositional magmatism in the Alisitos Group at Punta Cono, Baja California, Mexico. Sedimentology 34: 911-927.

IN PRESS

Willner, A.P.; Gerdes, A.; Masonne, H.J. 2008. History of crustal growth and recycling at the Pacific convergent margin of South America at latitudes 29°–36° S revealed by a U–Pb and Lu–Hf isotope study of detrital zircon from late Paleozoic accretionary systems. Chemical Geology 253: 114-129.

Willner, A.; Lottner, U.; Miller, H. 1987. Early Paleozoic structural development in the NW Argentine basement of the Andes and its implications for geodynamic reconstructions. *In* Gondwana six: Structure, tectonics and geophysics (McKenzie, G.D., editor). American Geophysical Union Monograph 40: 229-239.

Zimmermann, U.; Bahlburg, H. 2003. Provenance analysis and tectonic setting of the Ordovician deposits in the southern Puna basin, NW Argentina. Sedimentology 50: 1079-1104.

Zimmermann, U.; Niemeyer, H.; Meffre, S. 2010. Revealing the continental margin of Gondwana: the Ordovician arc of the Cordón de Lila (northern Chile). International Journal of Earth Sciences 99 (Suppl 1): S39–S56.

IN PRESS

Figure and table captions

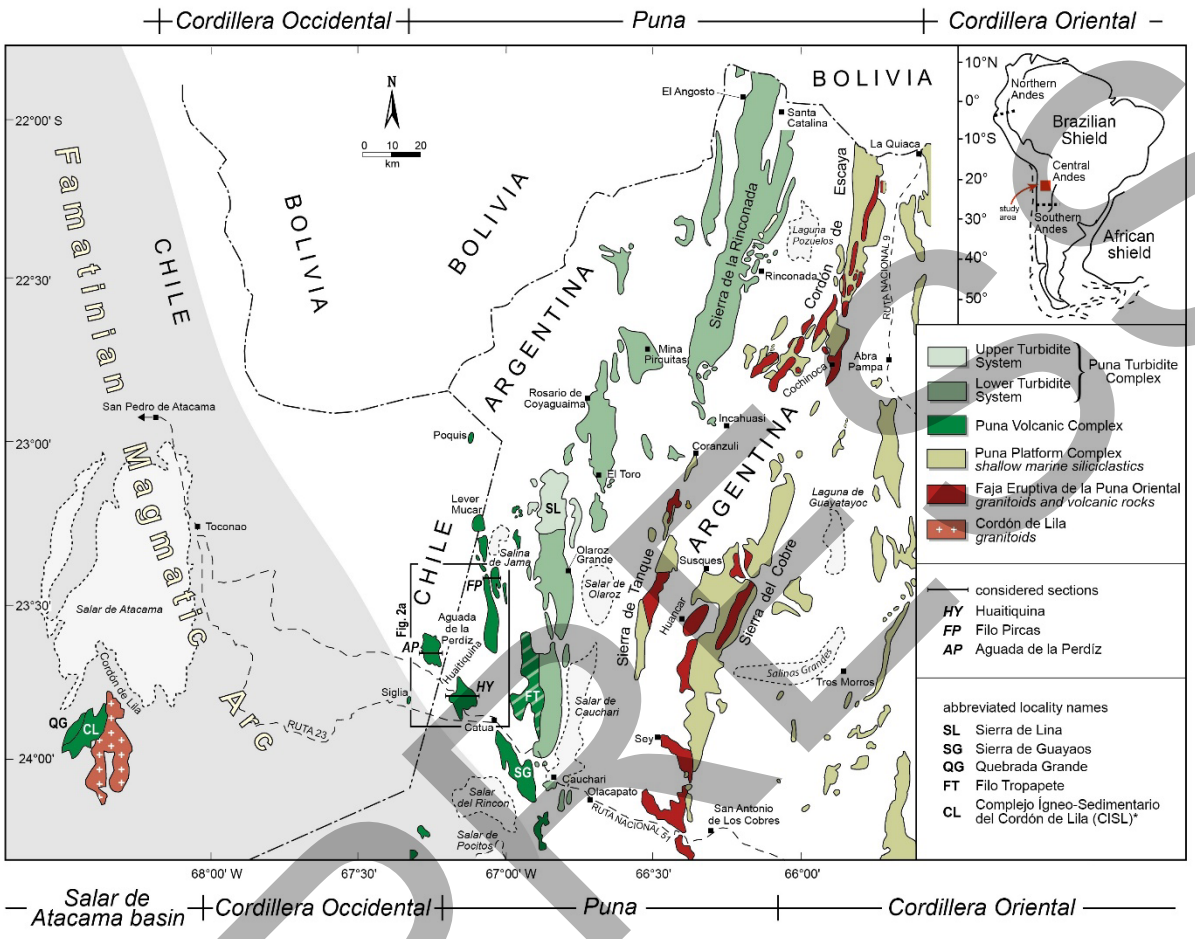

Figure 1. Outcrop map of Ordovician units in the Puna of northern Chile and northwestern Argentina, and in the Salar de Atacama Basin of northern Chile (modified from Bahlburg, 1990 and Augustsson et al., 2015). *sedimentary part.

IN PRESS

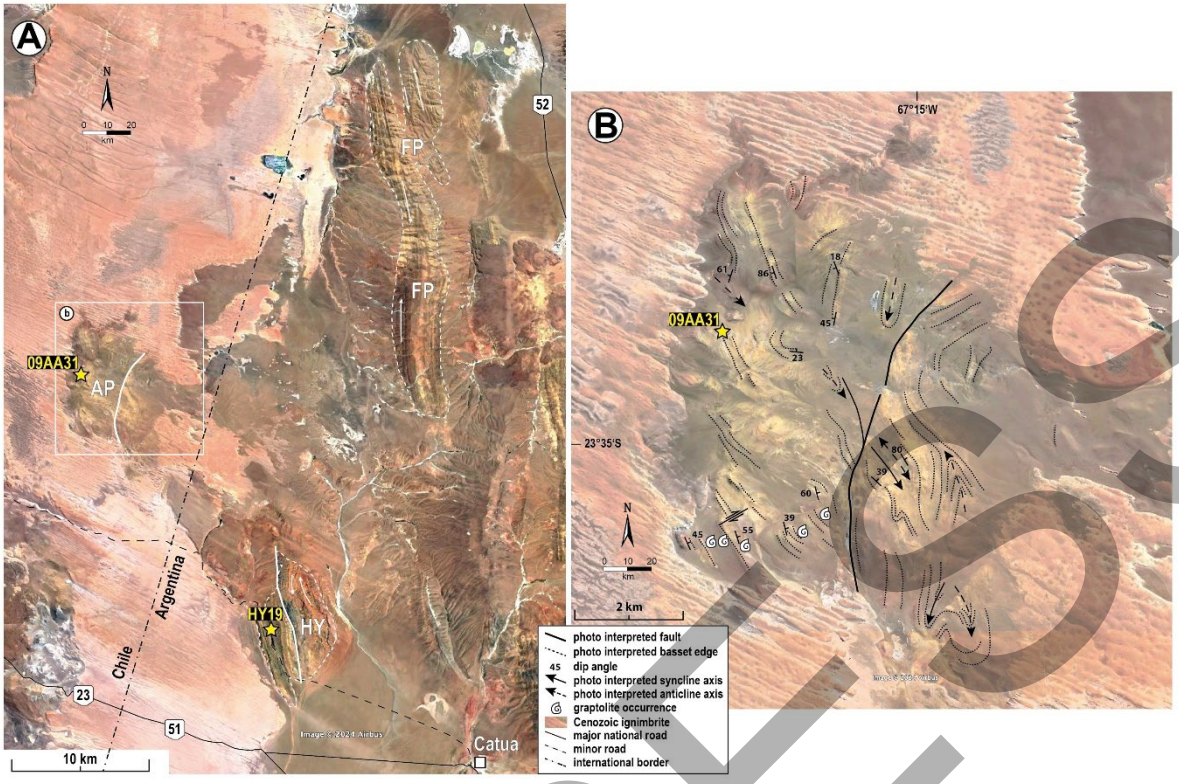

Figure 2. Google Earth satellite images (2025) of the Aguada de la Perdiz Formation. **A.** Overview of the Aguada de la Perdiz (AP), Huaitiquina (HY) and Filo Pircas (FP) localities. **B.** Interpretation of satellite image photolineations of the Aguada de la Perdiz outcrop, adapted from Breitkreuz (1986). Stars and labels indicate sampling localities, sample 09AA31: Einhorn et al. (2015), sample HY19: this contribution.

IN PRESS

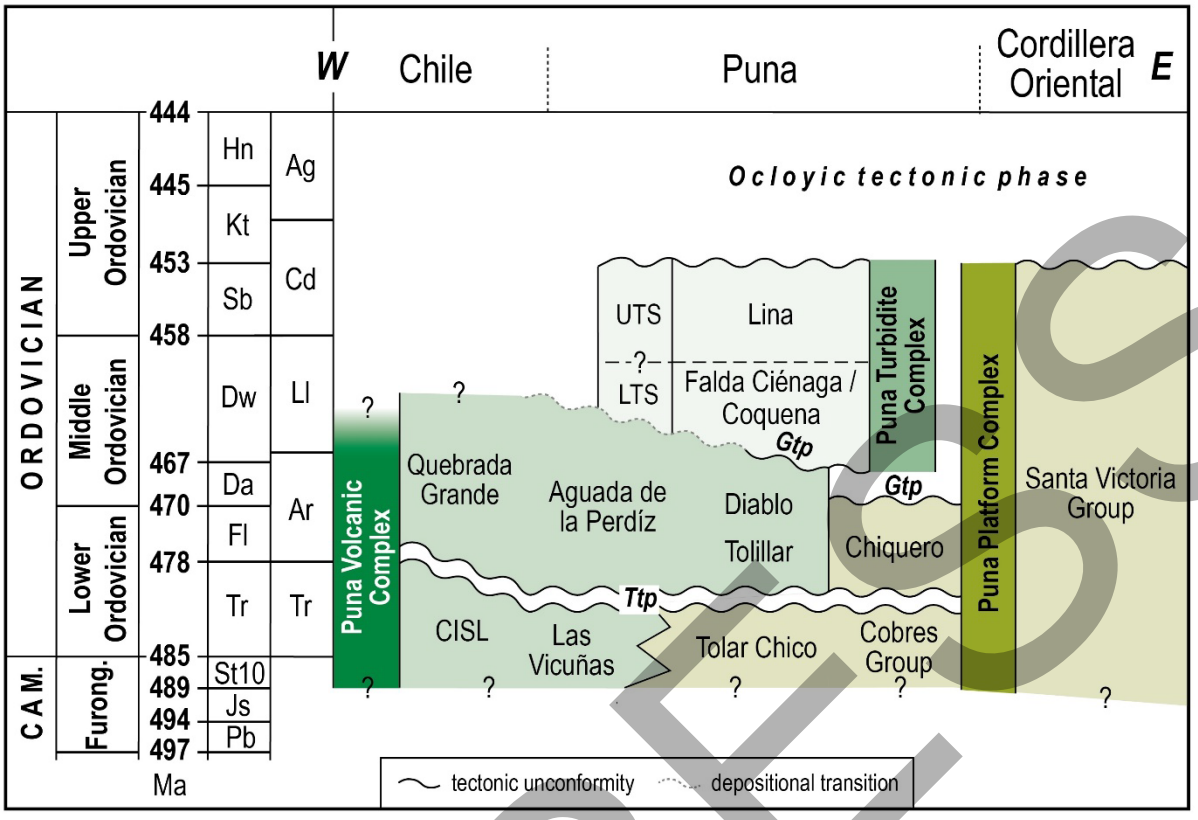

Figure 3. Uppermost Cambrian and Ordovician stratigraphy and formations of the Puna of northern Chile and northwestern Argentina (compiled and adapted from Schwab, 1973; Breitkreuz, 1986; Aceñolaza and Baldis, 1987; Bahlburg et al., 1990; Moya et al., 1993; González et al., 2007; Brussa et al., 2008; Moya, 2015; Toro and Herrera Sánchez, 2019; and Maletz, pers. comm., 2022, 2025). ICS chronostratigraphy according to Cohen et al. (2013, updated). Pb: Paibian; Js: Jiangshanian; ST10: unnamed Stage 10; Tr: Tremadocian; Fl: Floian; Da: Dapingian; Dw: Darriwilian; Sb: Sandbian; Kt: Katian; Hn: Hirnantian. Ar: Arenig; Ll: Llanvirn; Cd: Caradoc; Ag: Ashgill. Ttp: Tumbaya tectonic phase; Gtp: Guandacol tectonic phase. CISL: Complejo Ígneo-Sedimentario del Cordón de Lila; LTS: Lower Turbibidite System; UTS: Upper Turbidite System.

IN PRESS

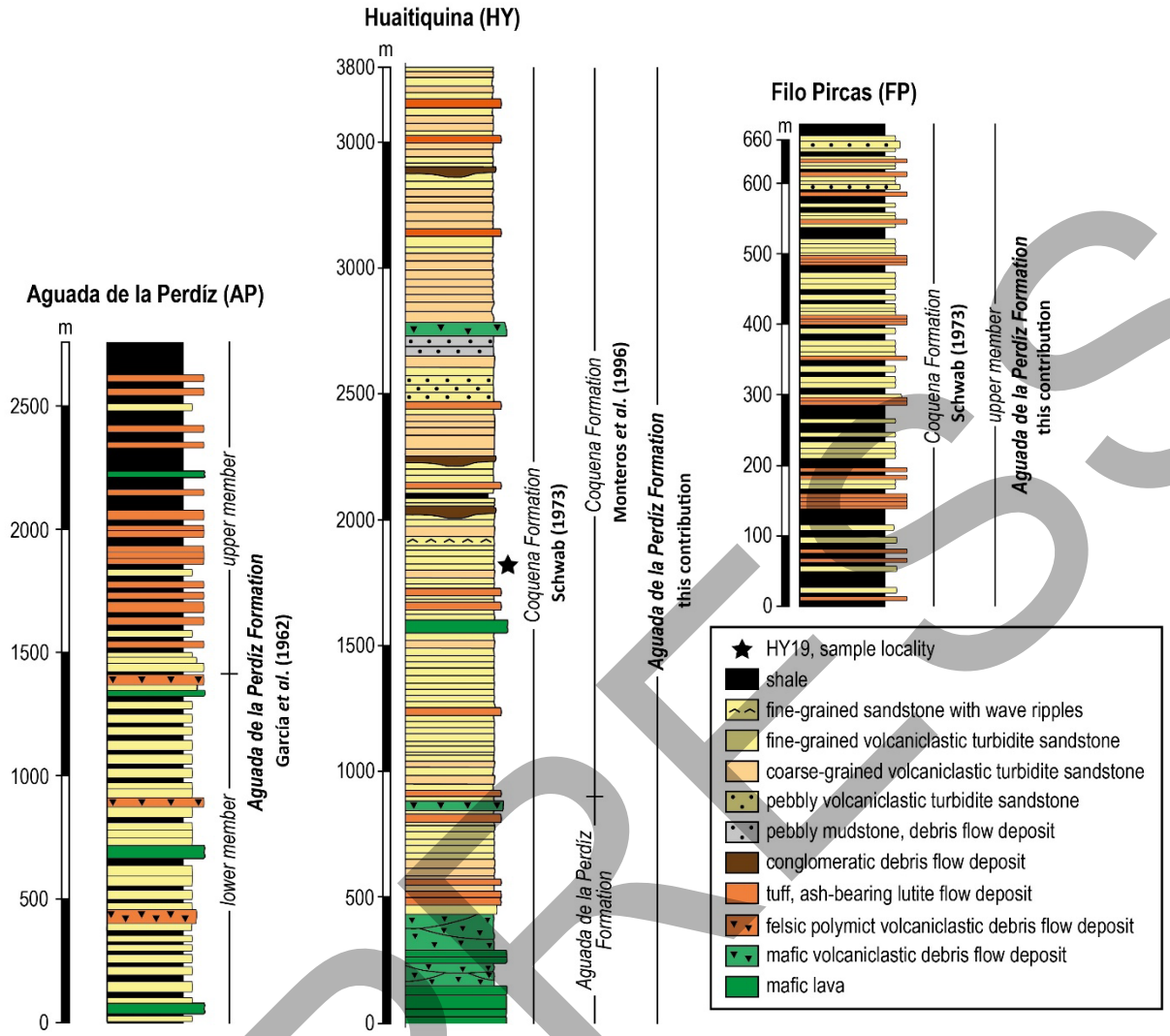

Figure 4. Schematic lithostratigraphic sections of the Aguada de la Perdiz Formation at the type locality (AP), and at Huaitiquina (HY) and Filo Pircas (FP). AP redrawn and modified from Breitkreuz (1986) and Bahlburg et al., (1990); HY redrawn and modified from Bahlburg (1990) and Monteros et al. (1996); FP redrawn from Bahlburg et al. (1990). The asterisk in HY marks the origin of detrital zircon sample HY19 shown in Figure 7.

IN PRESS

Figure 5. Outcrop pictures of the Aguada de la Perdiz Formation at the type locality (A-E) and at the Filo Pircas section (F-H). **A.** Outcrop overview with thin-bedded ash-bearing flow deposits of the upper member in foreground and Cenozoic ignimbrite cover in the middleground. **B.** Submarine rhythmic coarse-tail graded volcaniclastic turbidites, upper member (from Breitkreuz, 1986). **C-D.** Outcrop view and detail of lower member felsic volcaniclastic debris flow deposit with rafts of fine-grained ash-bearing flow deposits. **E.** Detail of upper member ash-bearing flow deposit showing cross-bedding. **F.** Outcrop overview. **G.** Thin-bedded ash-bearing flow deposits. **H.** Graded volcaniclastic turbidites (from Bahlburg, 1990).

UNDER PEER REVIEW

Figure 6. Outcrop pictures of the Aguada de la Perdiz Formation at the Hyuaitiquina locality. **A.** Overview of lower part of the section with alternating dark mafic lavas and debris flow deposits in the foreground, and red to light colored volcaniclastic turbidite sandstones and debris flow deposits in the background. **B.** Overview of upper part of the section with predominant volcaniclastic turbidite sandstones and debris flow deposits. **C.** Jointed basaltic-andesite lavas. **D.** Mafic hydroclastic breccia. **E.** Mafic volcaniclastic debris flow deposit (from Bahlburg, 1990). **F.** Pebbly volcaniclastic turbidite overlain by coarse-grained volcaniclastic turbidite sandstone. **G.** Sandstone with symmetrical wave ripples (dashed white line). **H.** Alternations of laminated and massive fine-grained turbidites; bed with pocket knife shows ball and pillow dewatering structures.

IN PRESS

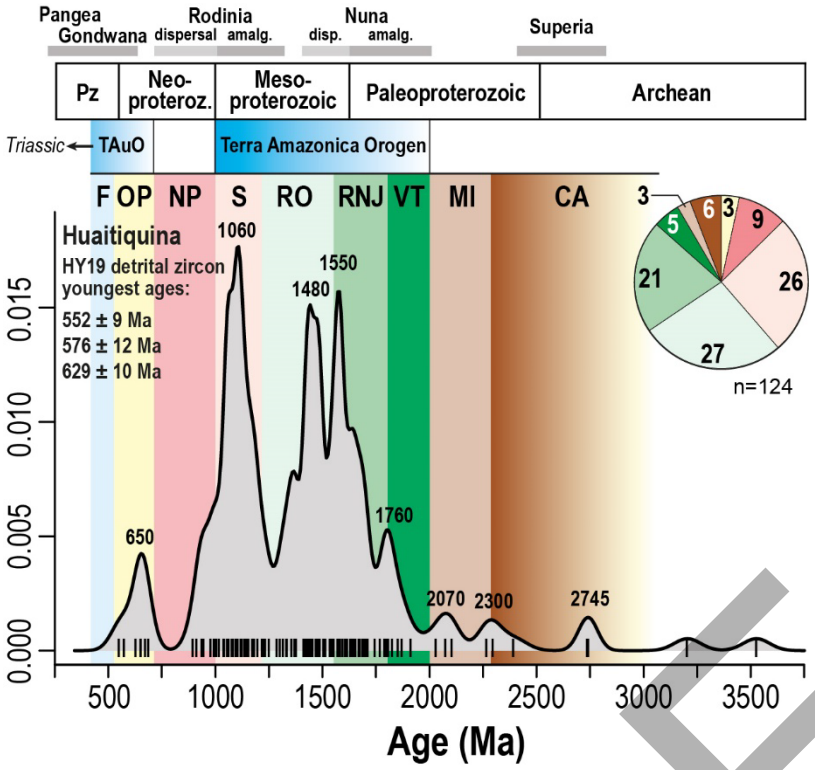

Figure 7. Kernel Density Estimates (KDE, bandwidth 25) of zircon U–Pb ages of detrital zircon in the lower Ordovician Aguada de la Perdiz Formation at Huaitiquina (HY19). Abbreviations of orogens and orogenic and tectonic cycles according to Bahlburg et al. (2025). TAuO: Terra Australis Orogen. CA: Central Amazonian; F: Famatinian; MI: Maroni-Itacaiunas (Transamazonian); NP: Neoproterozoic rifting; OP: Olmos-Pampean; RNJ: Río Negro-Juruena; RO: Rondonia-San Ignacio; S: Sunsás; VT: Ventuari-Tapajos. Pie chart gives the age distribution in percent of the main contributing source provinces.

Table 1. Graptolite faunas and stratigraphic ages of different outcrops of the Aguada de la Perdiz Formation, compiled from Fuenzalida (1957), García et al. (1962), Schwab (1973), Aceñolaza and Durand (1975), Pérez (1983), Breitkreuz (1986), Coira and Nullo (1989), Bahlburg et al. (1990), Gutierrez-Marco et al. (1996), Monteros et al. (1996), Benedetto et al. (2008), Toro et al. (2019, 2020), and Maletz (pers. comm., 2022, 2025). Conodonts at Huaitiquina from Toro et al. (2020). Graptolites and brachiopods of the Quebrada Grande Formation from González et al. (2007). For global stratigraphic stages see figure 3.

IN PRESS

914 **Supplementary material**

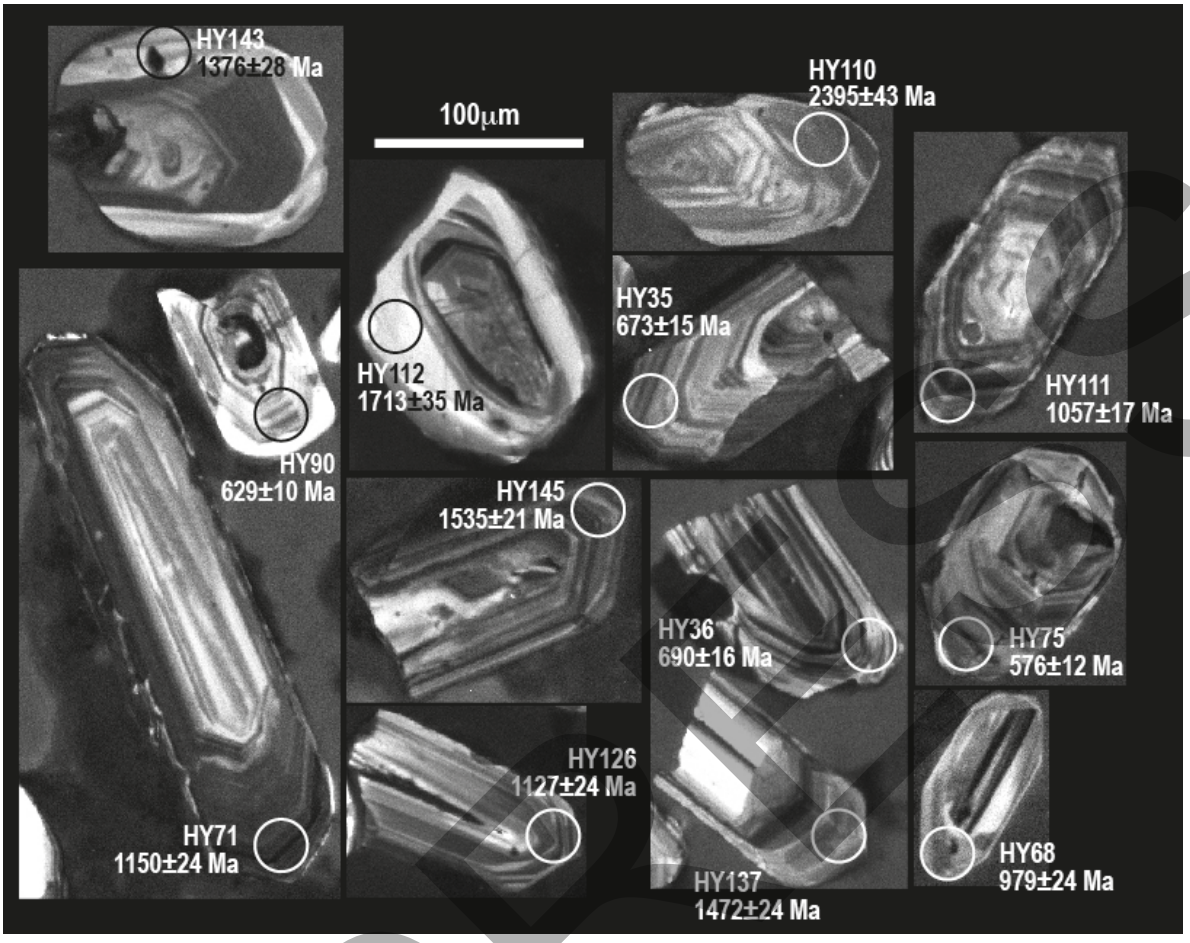

915

916 Supplementary Figure 1. Representative cathodoluminescence (CL) images of zircons
917 predominantly showing oscillatory zoning characteristic of a magmatic origin. The
918 circles indicate the positions of 25 μm diameter U–Pb isotope laser ablation spots.

919

920 Supplementary Table 1. Detrital zircon age data of sample HY19.

921

922

923

IN PRESS